Competition between ferromagnetic and antiferromagnetic ground states in multiferroic $BiMnO_3$ at high pressures

D. P. Kozlenko,[1] A. A. Belik,[2] S. E. Kichanov,[1] I. Mirebeau,[3] D. V. Sheptyakov,[4] Th. Strässle,[4] O. L. Makarova,[5] A. V. Belushkin,[1] B. N. Savenko,[1] and E. Takayama-Muromachi[2]

[1]*Frank Laboratory of Neutron Physics, JINR, 141980 Dubna, Russia*

[2]*International Center for Materials Nanoarchitectonics (MANA), National Institute for Materials Science (NIMS), 1-1 Namiki, Tsukuba, Ibaraki 305-0044, Japan*

[3]*Laboratoire Léon Brillouin, CEA-CNRS, CEA Saclay, 91191 Gif-sur-Yvette, France*

[4]*Laboratory for Neutron Scattering, Paul Scherrer Institut, ETH Zurich, CH-5232 Villigen, Switzerland*

[5]*Russian Research Center "Kurchatov Institute," 123182 Moscow, Russia*

(Received 30 March 2010; revised manuscript received 27 May 2010; published 2 July 2010)

The crystal and magnetic structures of $BiMnO_3$ were studied at high pressures up to 10 GPa by means of neutron diffraction in the temperature range 2–300 K. Three structural modifications, two monoclinic and one orthorhombic were found to exist in the pressure range studied and their structural parameters were determined. A suppression of the initial ferromagnetic state and formation of a new antiferromagnetic state with a propagation vector (1/2 1/2 1/2) was observed at $P \sim 1$ GPa, accompanied with the monoclinic-monoclinic structural transformation. Possible mechanisms of the pressure-induced magnetic transition and origin of magnetoelectric phenomena in $BiMnO_3$ are discussed.

DOI: 10.1103/PhysRevB.82.014401 PACS number(s): 75.25.−j, 61.50.Ks, 71.30.+h

I. INTRODUCTION

The perovskitelike complex manganese oxides $RMnO_3$ (R—rare-earth elements) and related compounds are well known for challenging physical phenomena, such as colossal magnetoresistance, insulator-metal transition, orbital and charge ordering, structural and magnetic phase separation, which have been extensively studied during last years.[1] Recently particular attention has been given to multiferroic phenomena observed in $RMnO_3$ (R=Tb,Dy,Gd,Bi) compounds.[2–6] In these materials, ferroelectricity coexists with a long-range magnetically ordered ground state of incommensurate or commensurate nature. This leads to interesting physics, such as the switching of electric polarization by magnetic field (very prospective for electronic devices), possible excitations of electromagnons, and promising many more effects awaiting to be unraveled.[2,4,7] Among $RMnO_3$ multiferroics, $BiMnO_3$ is a rare example of a compound with collinear ferromagnetic (FM) ground state (T_{FM}=100 K), possessing orbital order. The ferroelectric transition occurs at $T_{FE} \approx 770$ K $\gg T_{FM}$ and it is accompanied by a structural transformation from an orbitally disordered $C2$ to an orbitally ordered $C2/c$ monoclinic phase.[5,6,8,9] The origin of ferroelectricity in $BiMnO_3$ is generally related to a stereochemically active lone pair $6s^2$ of Bi^{3+} ions, which induces local structural distortions.[6]

Due to the centrosymmetric character of the $C2/c$ structure, the nature of the magnetodielectric anomaly[5] and ferroelectric hysteresis loop,[6] observed in $BiMnO_3$ in the vicinity of T_{FM}, remains unclear. A prominent magnetoelastic coupling due to partially frustrated magnetic interactions below T_{FM}, not leading to changes in the symmetry of the crystal structure and correlating with dielectric anomaly, was observed in neutron-diffraction study.[9] This implies that magnetoelectric properties should be related to structural distortions, breaking the average crystal structure symmetry at a local level. Subsequent theoretical calculations pointed out that a possible mechanism for inversion symmetry breaking is associated with a competition of nearest-neighbor FM and longer range antiferromagnetic (AFM) superexchange interactions.[10] These calculations have also shown that under certain conditions the AFM phase favoring magnetoelectric behavior is expected to emerge in $BiMnO_3$.

Recent magnetic susceptibility[11,12] and x-ray diffraction[13] measurements revealed a new magnetic phase transition at relatively moderate pressure $P \sim 1$ GPa accompanied by the structural phase transformation in $BiMnO_3$. These observations provided additional evidence of highly competing character of magnetic interactions in $BiMnO_3$ and indirect support to theoretical considerations.[10] However, the magnetic order symmetry and full set of the structural parameters of the high-pressure phase of $BiMnO_3$, important for further elucidation of the nature of its magnetoelectric properties, remain unknown. In this paper, the crystal and magnetic structures of $BiMnO_3$ were studied by neutron powder diffraction at high pressures up to 10 GPa.

II. EXPERIMENT

The compound $BiMnO_3$ was synthesized from a stoichiometric mixture of Bi_2O_3 (99.99%) and Mn_2O_3, which was placed in Au capsules and treated at 6 GPa in a belt-type high-pressure apparatus at 1383 K for 60–70 min. After heat treatment, the samples were quenched to RT, and the pressure was slowly released. The resultant samples were black powder. X-ray powder diffraction showed that the samples were single phase. Single-phase Mn_2O_3 was prepared by heating commercial MnO_2 (99.99%) in air at 923 K for 24 h. Bi_2O_3 was dried at 570 K before its use.

The crystal structure of $BiMnO_3$ was investigated using the high resolution powder diffractometer for thermal neutrons (HRPT) [14] at the SINQ neutron spallation source (Paul

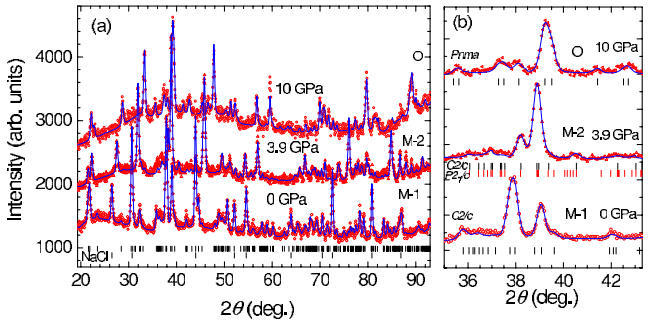

FIG. 1. (Color online) (a) Neutron diffraction patterns of $BiMnO_3$ measured at selected pressures and ambient temperature at HRPT diffractometer (PSI) for two monoclinic (M-1 and M-2) and orthorhombic (O) structural phases and processed by the Rietveld method. Experimental points and calculated profiles are shown. Ticks below represent calculated positions of nuclear peaks of ambient pressure monoclinic phase and NaCl used for pressure calibration. (b) Parts of neutron-diffraction patterns illustrating changes related to pressure-induced structural phase transitions. Ticks represent calculated positions of nuclear peaks of the M-1, M-2 (for the $C2/c$ and $P2_1/c$ structural models), and O phases.

Scherer Institute, Switzerland) combined with an opposed-anvil high-pressure setup for studies up to 10 GPa at ambient temperature.[15] The incident neutron wavelength was 1.494 Å. The Paris-Edinburgh high-pressure cell was used with a 4:1 volume mixture of fully deuterated methanol-ethanol as a pressure-transmitting medium. A TiZr encapsulated gasket of 70 mm^3 effective sample volume was used to attain nearly hydrostatic compression of the sample in the pressure range studied. Typical data collection times were about 15 h per pressure point. For the pressure determination, the known equation of state of NaCl, admixed to the sample in a 1:2 volume proportion, was used.[16]

The magnetic structure of $BiMnO_3$ was investigated with the G6.1 diffractometer at the Orphée reactor (Laboratoire Léon Brillouin, France) using a setup for high-pressure experiments.[17] The incident neutron wavelength was 4.74 Å. The sample with a volume of about 2 mm^3 was loaded into the sapphire-anvil high-pressure cell.[18] Several tiny ruby chips were placed at different points of the sample surface and the pressure was determined by a standard ruby fluorescence technique. Measurements of the pressure distribution on the sample yield typical pressure inhomogeneities of $\pm 10\%$. Diffraction patterns were collected in the pressure range 0–2 GPa and temperature range 2–120 K. Typical data collection times were about 5–7 h per pressure/temperature point. The diffraction data for both the crystal and magnetic structure were analyzed by the Rietveld method using the FULLPROF program.[19]

III. RESULTS

The characteristic neutron-diffraction patterns of $BiMnO_3$ measured at selected pressures up to 10 GPa and ambient temperature at the HRPT diffractometer (PSI) are shown in Fig. 1. At ambient conditions the monoclinic structure of $C2/c$ symmetry was detected. At pressures above 1 GPa, noticeable changes in the diffraction data were observed [Fig. 1(b)], evidencing a structural phase transition. From the data analysis it was found that the structure of the high-pressure phase of $BiMnO_3$ can also be described as monoclinic one with $C2/c$ symmetry but with different ratio of lattice parameters compared to the ambient pressure phase. In a recent x-ray diffraction study[13] the $P2_1/c$ symmetry was assumed for the crystal structure of this high-pressure phase, although no complete structural data were reported. This model can also describe experimental data quite well with nearly the same lattice parameters. However, comparison between the calculated reflections positions for the $C2/c$ and $P2_1/c$ models[20] and the experimental data has shown that all observed diffraction peaks with statistically significant intensity can be indexed within the higher $C2/c$ symmetry (Fig. 1). In addition, due to about twice increased number of structural parameters in the $P2_1/c$ model, it was impossible to obtain accurate values of all bond distances and angles. From these reasons, the $C2/c$ model was finally chosen for further data analysis. The structural parameters of two monoclinic phases of $BiMnO_3$ obtained from Rietveld refinement of diffraction data at selected pressures are listed in Tables I and II. At ambient pressure their values are close to those reported previously.[8,9] The pressure-induced structural transformation yields an increase in the a lattice parameter, monoclinic angle β, and a decrease in the b and c lattice parameters, while the unit-cell volume decreases (Fig. 2). In the ambient pressure monoclinic phase, the MnO_6 octahedra possess noticeable Jahn-Teller (JT) structural distortions, related to the long-range three-dimensional order between $d(3z^2-r^2)/d(3x^2-r^2)/d(3y^2-r^2)$ e_g orbitals.[8] The JT distortion parameter $\delta_{JT}=\sqrt{\frac{1}{3}\Sigma_i[(l_{Mn\text{-}O})_i-\langle l_{Mn\text{-}O}\rangle]^2}$ values of 0.138 and 0.140 for oxygen octahedra around Mn1 and Mn2 sites are about the same and comparable with that found for $LaMnO_3$ having two-dimensional $d(3x^2-r^2)/d(3y^2-r^2)$ e_g orbital order, $\delta_{JT}=0.114$.[21] In the high-pressure monoclinic phase, the oxygen octahedra around Mn2 site become less distorted in comparison with those around Mn1 sites. The relevant values at 3.9 GPa being δ_{JT} (Mn1)=0.112 and δ_{JT} (Mn2)=0.085, respectively.

At pressures above 8.5 GPa, the appearance of a second structural phase transition was observed in the diffraction data (Fig. 1). From the data treatment it was found that the crystal structure of the second high-pressure phase has the *Pbnm* orthorhombic symmetry, in agreement with a previous x-ray diffraction experiment.[13] The structural parameters of the orthorhombic phase of $BiMnO_3$ obtained from the Rietveld refinement of the diffraction data at pressure $P=10$ GPa are also listed in Table I. The JT distortion parameter has a value of $\delta_{JT}=0.107$ at 10 GPa. The pressure-induced orthorhombic phase of *Pbnm* symmetry was also previously observed in related Bi-based complex oxides, $BiFeO_3$, $BiScO_3$, and $BiCrO_3$.[13,22]

The pure magnetic part of the neutron-diffraction patterns of $BiMnO_3$ measured at selected pressures up to 2 GPa and $T=2$ K at G6.1 (LLB) is shown in Fig. 3. It was obtained by subtracting experimental data collected above magnetic ordering temperature ($T=120$ K) from those collected at low temperature. At ambient pressure below $T_{FM}\approx 100$ K an additional contribution to the intensity of diffraction peaks

TABLE I. Structural parameters of ambient pressure monoclinic phase and high-pressure monoclinic and orthorhombic phases of $BiMnO_3$ at high pressures and ambient temperature. The R_p and R_{wp} factors values are also given.

P (GPa)		a (Å)	b (Å)	c (Å)	β (deg)
0	Cell ($C2/c$)	9.5473(1)	5.6167(1)	9.8699(1)	110.66(2)
	Atom	x	y	z	
	Bi (8f)	0.1375(9)	0.2114(12)	0.1269(8)	
	Mn1 (4e)	0.0	0.219(4)	0.75	
	Mn2 (4d)	0.25	0.25	0.5	
	O1 (8f)	0.097(1)	0.173(2)	0.578(1)	
	O2 (8f)	0.145(1)	0.568(2)	0.366(1)	
	O3 (8f)	0.356(1)	0.547(2)	0.166(1)	
R_p=2.51%, R_{wp}=3.12%					
2.9	Cell ($C2/c$)	9.6130(1)	5.4402(1)	9.7952(1)	111.00(2)
	Atom	x	y	z	
	Bi (8f)	0.124(4)	0.240(4)	0.121(3)	
	Mn1 (4e)	0.0	0.230(8)	0.75	
	Mn2 (4d)	0.25	0.25	0.5	
	O1 (8f)	0.096(4)	0.217(6)	0.574(4)	
	O2 (8f)	0.139(4)	0.564(5)	0.396(4)	
	O3 (8f)	0.349(2)	0.535(3)	0.156(2)	
R_p=4.40%, R_{wp}=5.60%					
3.9	Cell ($C2/c$)	9.5951(1)	5.4275(1)	9.7754(1)	110.98(2)
	Atom	x	y	z	
	Bi (8f)	0.128(2)	0.239(2)	0.124(2)	
	Mn1 (4e)	0.0	0.231(8)	0.75	
	Mn2 (4d)	0.25	0.25	0.5	
	O1 (8f)	0.095(2)	0.200(3)	0.577(2)	
	O2 (8f)	0.141(2)	0.571(3)	0.401(2)	
	O3 (8f)	0.350(2)	0.537(3)	0.157(2)	
R_p=3.05%, R_{wp}=3.81%					
10	Cell ($Pbnm$)	5.4491(1)	5.5074(1)	7.5588(1)	
	Atom	x	y	z	
	Bi (4c)	0.988(3)	0.042(2)	0.25	
	Mn (4b)	0.5	0.0	0.0	
	O1 (4c)	0.106(3)	0.488(4)	0.25	
	O2 (8d)	0.677(3)	0.287(2)	0.045(2)	
R_p=2.96%, R_{wp}=3.69%					

(−2 0 2) and (1 1 1), located at $2\theta \approx 71°$ and 72° was observed (Fig. 3), corresponding to a formation of the ferromagnetic ground state. The ordered magnetic moments of Mn ions are oriented along the b axis and have value of $3.4(1)\mu_B$ at T=2 K, in agreement with previous neutron-diffraction studies at ambient pressure.[9,23]

At pressures above 1.0 GPa a decrease in the FM contribution to nuclear peaks and simultaneous appearance of new magnetic lines (1/2 1/2 1/2) and (−3/2 1/2 5/2)/(−5/2 −1/2 3/2)/(3/2 −1/2 3/2) located at $2\theta \approx 34.2°$ and 81.7° was observed in diffraction patterns at low temperature (Fig. 3), indicating a suppression of the initial FM state and formation of a new AFM ground state. From the analysis by the Rietveld method it was found that additional magnetic lines correspond to a formation of the AFM state with a propagation vector k=(1/2 1/2 1/2) and magnetic cell 2a, 2b, and 2c. The ordered Mn magnetic moments form FM planes perpendicular to (111) direction, with AFM coupling between adjacent planes (Fig. 4). Such an AFM arrangement resembles features of the A-type AFM one observed in classical JT system $LaMnO_3$ and related compounds with orthorhombic $Pnma$ crystal structure.[19] However, the e_g orbital order in $BiMnO_3$, relevant to characteristic distortions of MnO_6 octahedra, is of three-dimensional character (Fig. 4) and therefore quite different from that observed in $LaMnO_3$ with two-dimensional character.[19,24]

TABLE II. Bond distances and angles in different phases of $BiMnO_3$ at high pressures and ambient temperature.

P, GPa	0	2.9	3.9	10	
Space group	$C2/c$	$C2/c$	$C2/c$	$Pbnm$	
Mn1-O1, Å (×2)	2.215(1)	2.25(3)	2.20(2)	Mn-O1, Å (×2)	1.977(5)
Mn1-O2, Å (×2)	1.880(2)	1.93(3)	1.93(2)	Mn-$O2_a$, Å (×2)	1.88(1)
				Mn-$O2_b$, Å (×2)	2.14(1)
Mn1-O3, Å (×2)	2.002(2)	2.03(3)	2.02(2)		
Mn2-O1, Å (×2)	1.926(1)	1.88(3)	1.91(2)		
Mn2-O2, Å (×2)	2.238(1)	2.08(3)	2.08(2)		
Mn2-O3, Å (×2)	1.959(1)	1.89(3)	1.89(2)		
Mn1-O1-Mn2, deg	149.5(5)	150.5(7)	152.6(5)	Mn-O1-Mn, deg	145.8(5)
Mn1-O2-Mn2, deg	161.5(5)	159.9(7)	156.6(5)	Mn-O2-Mn, deg	148.3(5)
Mn1-O3-Mn2, deg	149.0(5)	151.8(7)	152.0(5)		

In magnetic structure refinements the ordered Mn magnetic moments were calculated using the scale factors of FM and AFM phases constrained to the scale factor of nuclear phase, taking into account the multiplication of the AFM unit-cell volume with respect to nuclear one. The similar values $\mu_{FM}=1.8(1)$ and $\mu_{AFM}=1.7(1)\mu_B$ at $P=1.0$ GPa and $T=2$ K were obtained. This implies comparable volume fractions of FM and AFM magnetic phases in assumption that absolute values of magnetic moments per Mn^{3+} ion are close in these phases. The ordering temperatures calculated from the temperature dependences of the magnetic moments (Fig. 5) are $T_{FM}=95(4)$ and $T_{AFM}=90(4)$ K at $P=1.0$ GPa for the coexisting FM and AFM phases, respectively. These values are comparable with those derived from magnetic susceptibility measurements at high pressure.[11] The qualitatively different character of the temperature dependences of the magnetic moments related to FM and AFM phases (Fig. 5) allows to exclude the alternative conical magnetic structure model.

With further pressure increase up to 1.8 GPa a coexistence of FM and AFM phases still persists (Fig. 3). The calculated values of the ordered magnetic moments and magnetic ordering temperatures are about the same as those at $P=1.0$ GPa within the experimental accuracy.

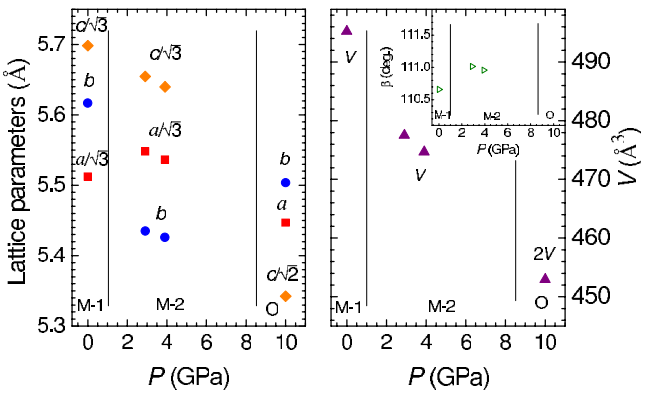

FIG. 2. (Color online) High-pressure behavior of lattice parameters and unit-cell volume in different phases of $BiMnO_3$.

IV. DISCUSSION

Let us consider the possible mechanisms of the observed pressure-induced change in the ground state from FM to AFM ordering, which occurs concomitantly with the structural phase transition, on the basis of Goodenough-Kanamori-Anderson rules for magnetic superexchange interactions.[25–27] In the magnetic structure of $BiMnO_3$ there are three nonequivalent nearest-neighbor superexchange interactions—Mn1-O1-Mn2 and Mn1-O2-Mn2 interactions of FM character between filled and empty e_g states and Mn1-O3-Mn2 interactions of AFM character between empty e_g states (Fig. 4). At ambient pressure FM superexchange interactions are dominant and the FM ground state is stabilized. At high pressure, in the AFM structure of $BiMnO_3$ the (111) planes are characterized be the presence of all three types of superexchange interactions, while they are coupled by only two types of interactions, namely, Mn1-O2-Mn2 and Mn1-O3-Mn2. Therefore, the FM-AFM change in the magnetic ground state can be qualitatively explained by a change in the balance between competing FM Mn1-O2-Mn2 and AFM

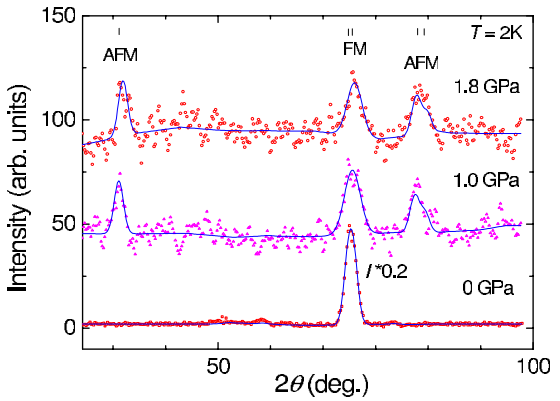

FIG. 3. (Color online) Pure magnetic part of neutron-diffraction patterns of $BiMnO_3$ at selected pressures and $T=2$ K processed by the Rietveld method. The experimental points and calculated profiles are shown. The characteristic magnetic peaks of FM and AFM phases are marked correspondingly.

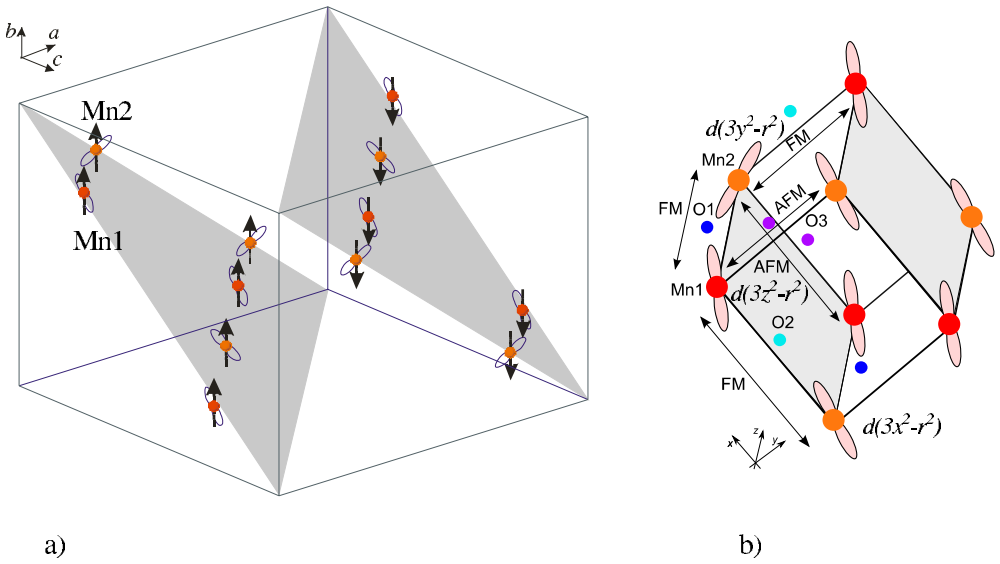

FIG. 4. (Color online) (a) The AFM structure of $BiMnO_3$ at high pressures above 1 GPa. The directions of ordered Mn magnetic moments and characteristic e_g orbital order are shown. (b) The competing magnetic interactions are illustrated with respect to perovskite subunit of the crystal structure.

Mn1-O3-Mn2 superexchange interactions in the favor of Mn1-O3-Mn2 ones. On the other hand in the (111) planes the Mn1-O1-Mn2 FM interactions remain dominant, leading to FM order within these planes. Inelastic neutron-scattering studies of related $RMnO_3$ compounds (R=La,Pr,Tb) have shown that superexchange integrals are mainly controlled by the Mn-O-Mn bond angle value while their dependence on the Mn-O distance is less pronounced.[28] The superexchange integrals between empty e_g states were found to follow the expected $J \sim \cos^2(\theta_{\text{Mn-O-Mn}})$ behavior while those between filled and empty e_g states exhibit much more pronounced variation with the Mn-O-Mn angle. A noticeable decrease in the Mn1-O2-Mn2 bond angle value from 161.5° to 156.6° occurs due to structural phase transformation between monoclinic phases at high pressure and ambient temperature, accompanied by the modification of the magnetic state of $BiMnO_3$ on cooling. Simultaneously, Mn1-O3-Mn2 bond angle value exhibits an opposite increase from 149° to 152°. As a result, a significant reduction in the Mn1-O2-Mn2 FM superexchange interaction integral is expected, contrasting to increase in the Mn1-O3-Mn2 AFM superexchange interaction. This effect explains qualitatively the observed FM-AFM magnetic phase transition. It is worth noting that in our considerations we neglected additional temperature-induced variation in the structural parameters on cooling in the vicinity of the magnetic phase transition since this effect is several times smaller in comparison with pressure-induced variation in their values.[9]

The FM to AFM modification of the magnetic ground state in $BiMnO_3$ occurs at a moderate pressure of about 1 GPa while both FM and AFM phases coexist up to 2 GPa. This implies relatively close energies of the FM and AFM states and supports the idea that magnetoelectric phenomena in $BiMnO_3$ may occur due to local inversion symmetry breaking by competing magnetic interactions.[9,10] However, our analysis shows that there is rather competition between nearest-neighbor FM and AFM superexchange interactions than one between nearest-neighbor and longer range interactions, as proposed in Ref. 10.

Due to technical restrictions we were able to perform low-temperature experiments in the limited pressure range up to 2 GPa only and the magnetic structure of the orthorhombic high-pressure phase of $BiMnO_3$, appearing above 8.5 GPa, remains unclear. For orthorhombic $RMnO_3$ compounds it has been experimentally shown that the in-plane magnetic superexchange interaction integral J_{ab} changes its sign from FM to AFM at a certain critical value of the Mn-O2-Mn bond angle $\theta_{\text{crit}} \approx 145°$.[29] The relevant value for $BiMnO_3$ at 8.5 GPa is $\theta_{\text{Mn-O2-Mn}} = 148.3° > \theta_{\text{crit}}$, so the A-type AFM ground state is expected to persist in the orthorhombic phase of $BiMnO_3$, similar to that of $LaMnO_3$ and possessing two-dimensional $d(3x^2-r^2)/d(3y^2-r^2)$ e_g orbital order.[22]

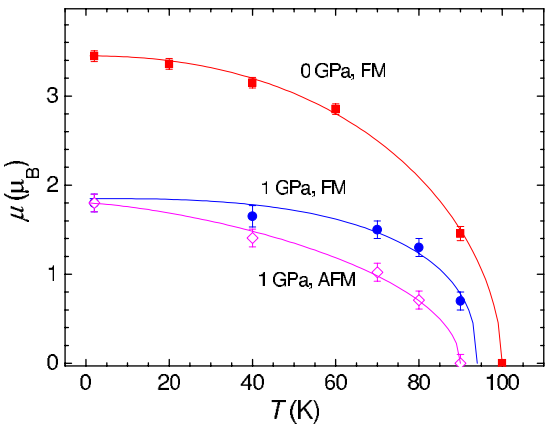

FIG. 5. (Color online) Temperature dependences of the ordered Mn magnetic moments for FM and AFM phases of $BiMnO_3$ at pressures 0 and 1 GPa. The solid lines represent interpolations by functions $\mu_{\text{FM(AFM)}} = [1-(T/T_{\text{FM(AFM)}})^{\alpha}]^{\beta}$. The obtained values of parameters are α=2.2(1) and β=0.51(5) for FM phase at P=0 GPa, α=2.4(1) and β=0.41(5) for FM phase at P=1 GPa, and α=1.4(1) and β=0.49(5) for AFM phase at P=1 GPa.

V. CONCLUSIONS

Our results demonstrate that the application of a relatively moderate pressure $P=1$ GPa leads to the suppression of the initial FM ground state ($T_{FM}=95$ K) and appearance of the AFM ground state ($T_{AFM}=90$ K) with the propagation vector $k=(1/2\ 1/2\ 1/2)$ in $BiMnO_3$, accompanied by the structural phase transformation between two monoclinic phases. The modified balance between FM and AFM superexchange interactions due to the underlying structural transformation is the possible reason for the observed magnetic phase transition. The highly competing character of these magnetic interactions results in a coexistence of FM and AFM ground states in the pressure range 0–2 GPa, and it supports the mechanism of magnetoelectric phenomena in $BiMnO_3$ caused by local inversion symmetry breaking (Ref. 10).

One more structural transition to an orthorhombic phase was observed at pressures above 8.5 GPa. A comparison between the structural parameters of $BiMnO_3$ and those of related orthorhombic $RMnO_3$ compounds implies that the *A*-type AFM ground state is expected to form in the orthorhombic phase.

ACKNOWLEDGMENTS

The work has been supported by the RFBR under Grant No. 09-02-00311-a, Grant of the President of the Russian Federation, Grant No. MD-696.2010.2, and state Contract No. 02.740.11.0542. The financial support from LLB is gratefully acknowledged. This work is partially based on experiments performed at the Swiss spallation neutron source SINQ, Paul Scherrer Institute, Villigen, Switzerland.

[1] *Colossal Magnetoresistance Oxides*, edited by Y. Tokura (Gordon and Breach, New York, 2000).
[2] T. Kimura, T. Goto, H. Shintani, K. Ishizaka, T. Arima, and Y. Tokura, Nature (London) **426**, 55 (2003).
[3] T. Goto, T. Kimura, G. Lawes, A. P. Ramirez, and Y. Tokura, Phys. Rev. Lett. **92**, 257201 (2004).
[4] S.-W. Cheong and M. Mostovoy, Nature Mater. **6**, 13 (2007).
[5] A. Moreira dos Santos, S. Parashar, A. R. Raju, Y. S. Zhao, A. K. Cheetham, and C. N. R. Rao, Solid State Commun. **122**, 49 (2002).
[6] T. Kimura, S. Kawamoto, I. Yamada, M. Azuma, M. Takano, and Y. Tokura, Phys. Rev. B **67**, 180401(R) (2003).
[7] A. Pimenov, A. A. Mukhin, V. Yu. Ivanov, V. D. Travkin, A. M. Balbashov, and A. Loidl, Nat. Phys. **2**, 97 (2006).
[8] A. A. Belik, S. Iikubo, T. Yokosawa, K. Kodama, N. Igawa, S. Shamoto, M. Azuma, M. Takano, K. Kimoto, Y. Matsui, and E. Takayama-Muromachi, J. Am. Chem. Soc. **129**, 971 (2007).
[9] E. Montanari, G. Calestani, L. Righi, E. Gilioli, F. Bolzoni, K. S. Knight, and P. G. Radaelli, Phys. Rev. B **75**, 220101(R) (2007).
[10] I. V. Solovyev and Z. V. Phelkina, New J. Phys. **10**, 073021 (2008).
[11] C. C. Chou, S. Taran, J. L. Her, C. P. Sun, C. L. Huang, H. Sakurai, A. A. Belik, E. Takayama-Muromachi, and H. D. Yang, Phys. Rev. B **78**, 092404 (2008).
[12] C. C. Chou, C. L. Huang, S. Mukherjee, Q. Y. Chen, H. Sakurai, A. A. Belik, E. Takayama-Muromachi, and H. D. Yang, Phys. Rev. B **80**, 184426 (2009).
[13] A. A. Belik, H. Yusa, N. Hirao, Y. Ohishi, and E. Takayama-Muromachi, Inorg. Chem. **48**, 1000 (2009).
[14] P. Fischer, G. Frey, M. Koch, M. Koennecke, V. Pomjakushin, J. Schefer, R. Thut, N. Schlumpf, R. Buerge, U. Greuter, S. Bondt, and E. Berruyer, Physica B **276-278**, 146 (2000).
[15] S. Klotz, Th. Strässle, G. Rousse, G. Hamel, and V. Pomjakushin, Appl. Phys. Lett. **86**, 031917 (2005).
[16] J. M. Brown, J. Appl. Phys. **86**, 5801 (1999).
[17] I. N. Goncharenko, I. Mirebeau, P. Molina, and P. Boni, Physica B **234-236**, 1047 (1997).
[18] I. N. Goncharenko, V. P. Glazkov, A. V. Irodova, O. A. Lavrova, and V. A. Somenkov, J. Alloys Compd. **179**, 253 (1992); I. N. Goncharenko, High Press. Res. **24**, 193 (2004).
[19] J. Rodríguez-Carvajal, Physica B **192**, 55 (1993).
[20] *International Tables for Crystallography*, edited by T. Hahn (Springer, Dordrecht, The Netherlands, 2005), Vol. A, pp. 184–192.
[21] L. Pinsard-Gaudart, J. Rodríguez-Carvajal, A. Daoud-Aladine, I. Goncharenko, M. Medarde, R. I. Smith, and A. Revcolevschi, Phys. Rev. B **64**, 064426 (2001).
[22] R. Haumont, P. Bouvier, A. Pashkin, K. Rabia, S. Frank, B. Dkhil, W. A. Crichton, C. A. Kuntscher, and J. Kreisel, Phys. Rev. B **79**, 184110 (2009).
[23] A. Moreira dos Santos, A. K. Cheetham, T. Atou, Y. Syono, Y. Yamaguchi, K. Ohoyama, H. Chiba, and C. N. R. Rao, Phys. Rev. B **66**, 064425 (2002).
[24] J. Rodríguez-Carvajal, M. Hennion, F. Moussa, A. H. Moudden, L. Pinsard, and A. Revcolevschi, Phys. Rev. B **57**, R3189 (1998).
[25] J. B. Goodenough, *Magnetism and the Chemical Bond* (Interscience, New York, 1963).
[26] J. Kanamori, J. Phys. Chem. Solids **10**, 87 (1959).
[27] P. W. Anderson, Phys. Rev. **115**, 2 (1959).
[28] R. Kajimoto, H. Mochizuki, H. Yoshizawa, H. Shintani, T. Kimura, and Y. Tokura, J. Phys. Soc. Jpn. **74**, 2430 (2005).
[29] B. Dabrowski, S. Kolesnik, A. Baszczuk, O. Chmaissem, T. Maxwell, and J. Mais, J. Solid State Chem. **178**, 629 (2005).